Reflection of sound by Sonic Crystals: an application to the aerospace engineering

L.M. Garcia-Raffi[1], L.J. Salmerón-Contreras[1],

I. Herrero-Durá[2], R. Picó[2], J. Redondo[2], V.J. Sánchez-Morcillo[2],

A. Cebrecos[3], N. Jiménez[3], V. Romero-García[3]

K. Staliunas[4]

[1] Instituto Universitario de Matemática Pura y Aplicada, Universitat Politècnica de València, Valencia, Spain
lmgarcia@mat.upv.es, luisalco@epsg.upv.es
[2] Instituto de Investigación para la Gestión Integrada de Zonas Costeras, Universitat Politècnica de València, Valencia, Spain
ivherdu@epsg.upv.es, rpico@fis.upv.es, fredondo@fis.upv.es, victorsm@fis.upv.es
[3] Laboratoire d'Acoustique de l'Université du Maine (LAUM). Le Mans, France.
alejandro.cebrecos@univ-lemans.fr, noe.jimenez@univ-lemans.fr, Vicente.Romero@univ-lemans.fr
[4] ICREA. Universitat Politècnica de Catalunya (UPC). Terrassa, Spain.
kestutis.staliunas@icrea.cat

Abstract
From the acoustical point of view one of the most extreme events is the lift-off of a rocket. In such events, an enormous amount of energy is liberated in the form of acoustic waves that are reflected in the launch pad, coming back over the rocket and affecting both the rocket and the load contained in the fairing. Here we propose a possible solution to reduce the sound pressure level in the area of the spacecraft-launcher: placing structures based on Sonic Crystals (SCs) at the launch pad to control waves reflecting on it. In this work preliminary results, in linear regime and without considering dissipation, about the use of SCs to control the reflected waves in a broadband range of frequencies are presented. This proof of concept is experimentally tested in a sub-scale system, that works at ultrasonic frequencies in water. Different types of SCs and different geometries of the reflecting backing are tested. In particular, geometries that mimic that of the VEGA's launch pad of the European Spatial Agency (ESA).

Keywords: Sonic Crystals, reflection, noise reduction, aerospace, launch pad.

PACS no. 43.20.+g, 43.50.+y, 43.35.+d,

1 Introduction

In aerospace engineering, ignition and lift-off of a rocket are extremely violent events in which a huge amount of energy is liberated, one part of it in the form of acoustic waves [1]. Very high amplitude acoustic waves are generated by the engine and the supersonic jet of hot gases produced by it. Waves are reflected in the launch pad, coming back to the launch vehicle and inducing an important acoustic load in a broad frequency range. This acoustic load has a direct incidence on the rocket and the payload

in the fairing [2-6]. In fact, it is a limiting parameter for the design of some structural parts in satellites. Several strategies have been used recently to mitigate this problem. Some of them aim to act in the fairing by using absorbing coverings, dampers or active materials. Less attention has been paid to strategies directly addressed to reduce the pressure level at the launch pad. The most employed is based in a water deluge. An important flow of water is injected around the launch pad with the double purpose of cooling and absorbing sound (water sound suppression). However, the use of water has drawbacks as corrosion and damage on structures present in the launch pad.

Up to now, the design of launch pads has been mainly addressed to exhaust the hot gases and no attention has been paid to its acoustical design. A different case corresponds to the construction of new launch pads. For instance, a new design in Japan ([7]) optimize the channels for exhaustion of gases in order to disperse the sound. A different problem consists of designing solutions to modify the reflection of sound in launch pads in service where several restrictions must be respected. The latter is considered in this work where the problem of the reflection of sound in the VEGA's launch pad is studied (see Figure 1). Our approach consists on the modification of the acoustic response on the launch pad using Sonic Crystals.

Figure 1: VEGA's launch pad. The channels for exhaust gases are observed below the rocket.

Sonic crystals consist of a periodic array of acoustically rigid elements (scatterers) embedded in a fluid host medium as air or water. One of the most celebrated properties of the SCs is that they present Band Gaps (BG), that is, ranges of frequencies in which propagation is evanescent (Bragg condition). There exists an extensive literature about SCs but probably the less studied aspect is their behaviour in reflection [8]. Other appealing features of SCs are their permeability to the flux of fluids [9], a feature compatible to existing solutions as water deluge. Our purpose is to study the possibility of placing such structures at the VEGA's launch pad. In Section 2 the experimental setup is described, including the tested structures . In Section 3 the analysis of the results is presented and finally conclusions are presented in Section 4.

2 Experimental measurements of noise reduction with scaled mock-ups

In this section the experimental setup, the SCs and the mock-ups of the launch pad (that we have called "backings") performed to evaluate the action of the SCs placed at the launch pad are presented. All

measurements are made in the linear regime, i.e., nonlinear and dissipation effects are not under consideration in this study.

2.1 Experimental setup

The problem, as considered in this preliminary step, is scalable. Hence, a characteristic dimension can be considered initially and rescaled all the parameters on demand.. The characteristic dimension is chosen to work in the range of frequencies of our source and structures designed for the test. Experimental measurements were carried out in a water tank at frequencies corresponding to the ultrasonic regime. Some limitations of the study are noted: dissipation in air and water is different and the relative size of the different elements in the setup (the source, the SC and the backings) is different than the real ones at the launch pad.

The acoustic source used is an ultrasonic transducer from the firm Olympus Panametrics, model A301S, with a 25,4 mm in diameter and a resonant frequency f_0 = 500 kHz, suitable to work in the desired range of frequencies in the experiments, which is [200-800] kHz. The receiver is a miniature probe hydrophone from the firm Reson, model TC4038, specifically designed as a standard reference hydrophone for high frequencies, in the range [10-800] kHz. Besides, it accounts for an omnidirectional directivity. Both emitter and receiver have linear responses in the range of frequencies and amplitudes used in the experiment. The hydrophone is mounted in a robotized system installed in a water tank and allows to capture the signal in every point, as depicted schematically in Figure 2(a).

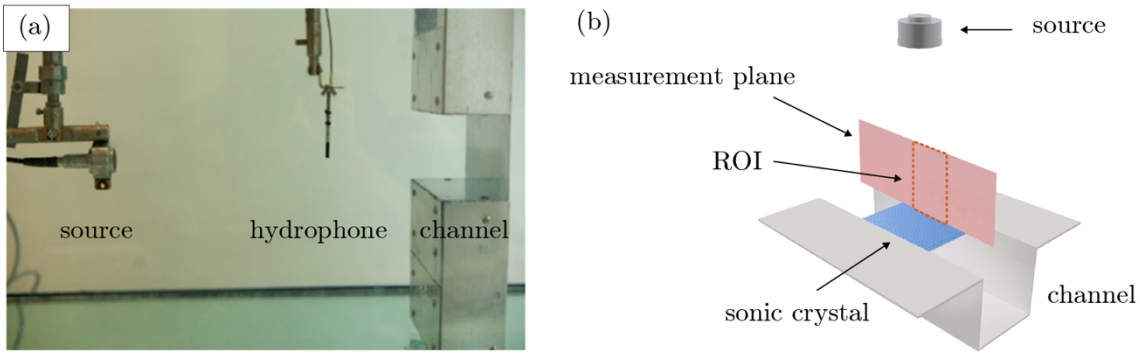

Figure 2: (a) Picture of the experimental setup, showing the relative position between the source, the hydrophone and a mock-up of the launch pad (b) Scheme of the measurements, showing the planes considered: dashed line shows the region of interest (ROI) used for spatial integration of the acoustic field in the analysis.

SCs used in the experiments are fabricated by Selective Laser Melting (SLM), an Additive Manufacturing (AM) process where a three-dimensional object is built layer by layer by laser scanning over a pre-deposited powder bed (see Figure 3). Structures were built in Titanium. The scatterers are square rods being the length of the edge L_SH=0,9 mm, L_SL=0,45 mm, L_TH=0,8 mm and L_SH=0,45 mm and the lattice constant is a=1.45 mm for all the structures. With these numbers, for both types of unit cell, square and triangular, two structures, one of low filling fraction and another of high filling fraction are considered. All structures present a pseudo band gap in the frontal direction (ΓX) except the structure TH (Figure 3 (d)) that presents a full band gap.

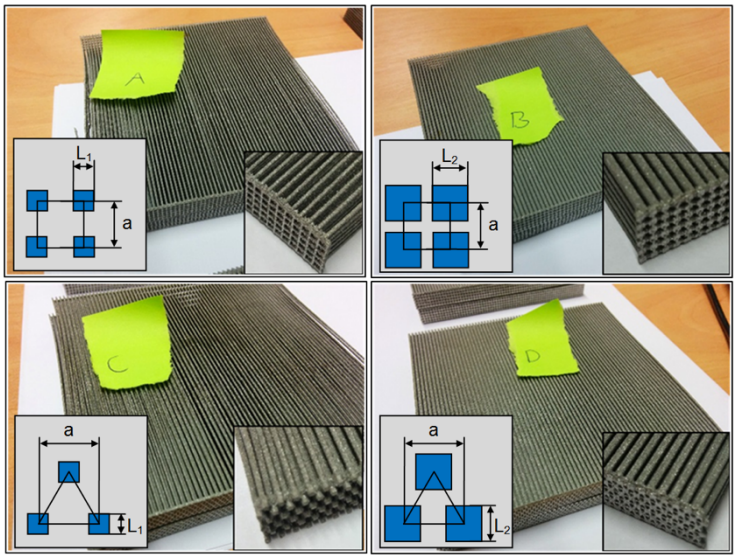

Figure 3: SCs built to be placed at the mock-up of the VEGA's launch pad. Insets represent the corresponding unit cell. a) Square lattice-Low filling fraction, SL, b) Square lattice-High filling fraction, SH, c) Triangular lattice-Low filling fraction, TL and d) Triangular lattice-High filling fraction, TH.

Figure 4 illustrates the different profiles of the mock-ups of the VEGA's launch pad considered as models of the channels for exhausting gases (real channels can be seen in Figure 1). The generic backing simulates a straight channel with a flat bottom, as shown in Figure 4 (a). In order to study the SCs analyzed in this work, we have compared their reflection properties with those of two reference elements:

1. A flat reflector with the same dimensions as the SC, depicted in Figure 4 (b),
2. A flat perforated reflector with the same dimensions as the SC, shown in Figure 4 (e).

Either the SCs or the reference elements will be placed over two different backings:

- A flat backing, as shown in Figure 4 (a),
- A W-shape backing, as depicted in Figure 4 (d).

The impulse response measurement technique. ([10]) is used to measure the reflected field by the SCs. This technique allows to separate incident and reflected waves by simply windowing in the time domain, . A sine-sweep signal $x(t)$ with increasing frequency is generated and emitted by the transducer and the response signal $y(t)$ is captured by the receiver. Then, the impulse response $h(t)$ is obtained by a convolution of the inverse of the input signal and the signal y(t),,

$$h(t) = x^{-1}(t) * y(t). \quad (1)$$

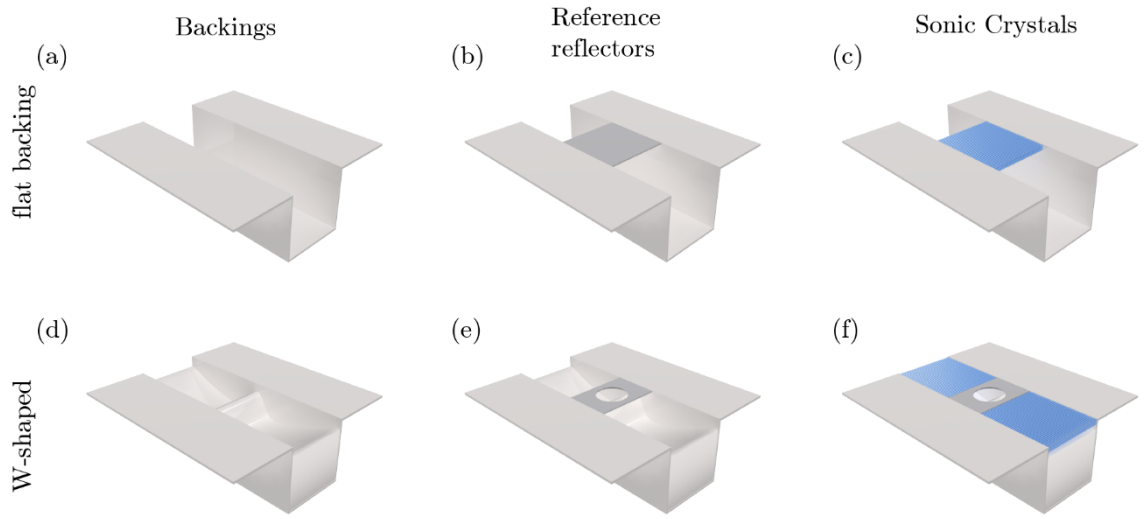

Figure 4: Design of the different launch pad mock-ups considered in this work

2.2 Definition of parameters

For the present study, the definition of some parameters used in other context is adapted to the case of reflection of waves. For instance, a common magnitude used to characterize linear system in transmission is the Insertion loss (IL), the loss of signal power resulting from the insertion of a device in a transmission line. In the context of acoustics, the IL is defined as the difference in sound pressure levels measured at a given location before and after a barrier or silencer is installed. This measurement provides a direct indication of the improvement provided by insertion of a structure between the noise source and the listener as a reduction of the transmitted acoustic energy. In our problem the source (the rocket engine) and the receiver (the rocket itself) are placed at the same side of the launch pad that reflects the acoustic energy. Hence, the Insertion Loss is redefined here to characterize the differences in the field reflected at the launch pad as a consequence of the placement of the different SCs. If P_1 and P_2 are the total pressure fields in two different configurations, the insertion loss is:

$$IL(dB) = 10\, Log_{10}\left(\frac{|P_1|^2}{|P_2|^2}\right). \tag{2}$$

The pressure field is integrated in frequency resulting in a map of the spatial distribution of the IL in a predetermined region in front of the structures, as shown in Figure 5. Similarly, a spatial integration of the pressure field is performed in a region called Region of Interest (ROI), depicted as a dashed rectangle in Figure 2 (b). This integration give rise to the IL distribution in frequency bands, as shown in Figure 6.

The Overall Sound Pressure Level (OASPL) is calculated as the total energy contained in the spectrum obtained by integration over all resolved frequencies, expressed in dB. In general, if the total energy (incident and reflected) of two different different configurations is compared, the OASPL is related to the IL by:

$$OASPL_1 - OASPL_2 = IL(dB), \tag{3}$$

The OASPL will be the magnitude used to compare the experimental results with the situation in the real launch pad.

3 Analysis of the reflected field by SC at the launchpad

In this Section experimental results and are presented. Two configurations are analyzed: using a single SC, as depicted in Figure 4(c), and using two identical SCs placed symmetrically, as shown in Figure 4(f).

In the configurations using a single SC, the comparison is made between the total field measured with the SC and the one measured with a flat reflector placed at the same position (Figure 4(c) and 4(b) respectively). Figure 5 shows the spatial distribution of IL corresponding to the four SC samples and IL integrated in frequency. The transducer is located at the top of the map (z = 0 mm), while the SC is located at the bottom of the image. As a result of placing the SC at the mock-up of the launch pad, as in Figure 4(c), the total field is lower than the total field corresponding to a flat reflector at the same position, as in Figure 4(b), i.e., the acoustic energy in the measured region is decreased. IL is positive on the central area of the ROI (red dashed rectangle in Figure 2(b)) that implies the spreading of the acoustic energy, i.e., a single SC produces a remarkable effect in comparison with a flat reflector placed at the same position, which produces a specular reflection.

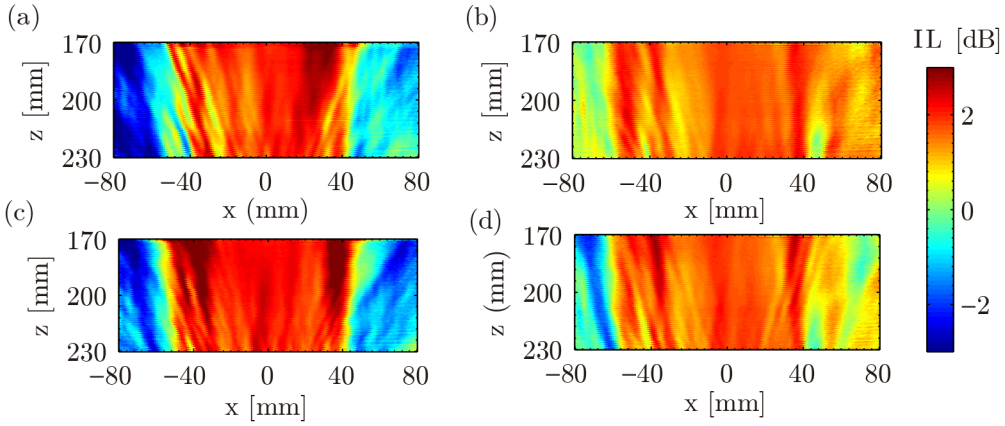

Figure 5. Spatial distribution of the insertion loss (IL). (a) SC-SL, (b) SC-SH, (c) SC-TL, (d) SC-TH.

In order to clarify the effect of SCs and quantify the total field reduction, IL values are calculated performing a spatial integration of the total field over the ROI (Figure 6). Values are presented in frequency bands and an overall global value is calculated (the red bar at the right side in every plot). A global IL value of around 2 dB is observed for all samples. Also, a typical behaviour of all structures is that lower values of IL are observed at band gap frequencies (500 kHz), that is, for frequencies in the band gap SCs behave as a reflector, as expected.. A closer look to results in Figure 5 shows that the factor with more influence is the filling fraction, where the highest IL values are found for the structures with low filling fraction.

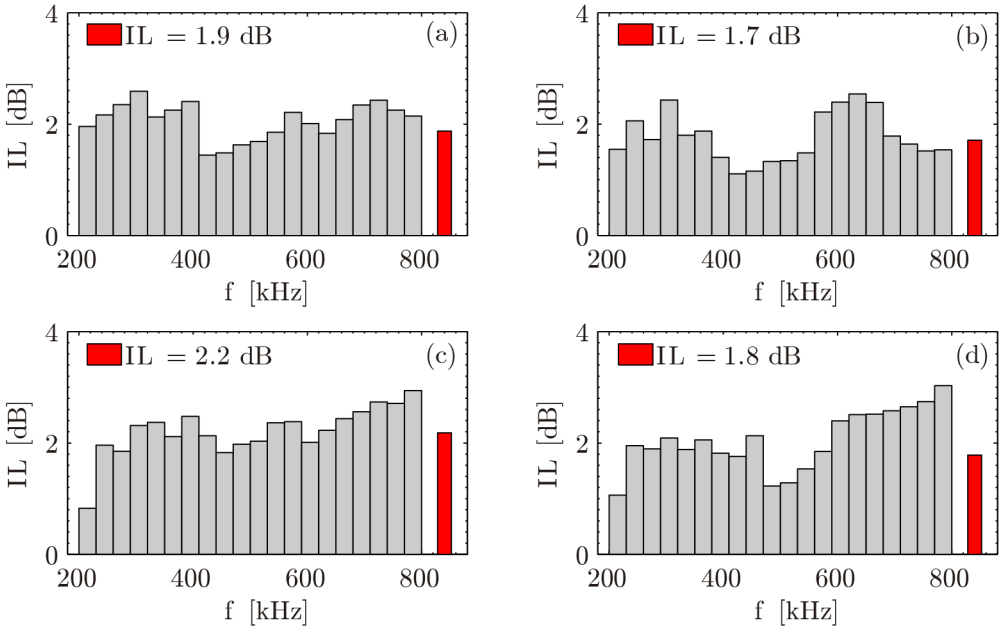

Figure 6: IL integrated on an area of 60 × 30 mm^2 (a) SC-SL, (b) SC-SH, (c) SC-TL, (d) SC-TH. The inset of the red bar represents and additional integration in frequency.

As shown in Figure 6, the structure with low filling fraction and triangular unit cell is the best within. This can be understood in terms of the band structures of the four crystals. The widest band gap corresponds to the structures with high filling fraction. Hence, the closer the behaviour to a flat rigid surface, the worse in scattering and diffusing the incident waves is the crystal. Focusing on the low filling fraction structures, the band gap in the case of the triangular lattice covers a narrower interval of frequencies than in the case of the square lattice.

OASPL results are presented for the best configuration, the sonic crystal with triangular unit cell and low filling fraction (SC-TL). Considering the existing OASPL data corresponding to the real launch pad and, although a direct comparison cannot be made, results presented here can be rescaled in order to predict the influence of the SCs. One drawback of this comparison is that in our experimental setup the frequency bandwidth of the transducer is limited to two octaves. Figure 7 shows the comparison between the OASPL of the actual launch pad (gray) and the OASPL predicted for a hypothetical structure formed by a channel with a SC. A reduction is noted in agreement with the results shown previously in Figures 5 and 6. This reduction is close to 2 dB that represents a reduction of the 37% per cent of the acoustic energy. In a real situation where the SC acts over the whole noise spectrum, it is expected that reduction of the OASPL is expected to be, in general, higher than the estimated here.

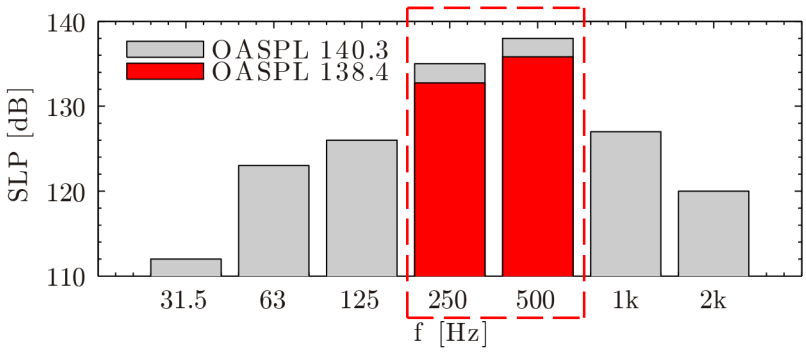

Figure 7: OASPL: Comparison between the launch pad and the configuration SC-TL

Finally, the closest configuration to the real launch pad is presented. This corresponds to Figure 4 (f), where two SCs with triangular unit cell and low filling fraction are placed symmetrically. The comparison is made with the case shown in Figure 4 (e), a new W-shaped backing at the bottom of the channel and a perforated flat reflector that mimics the platform where the rocket is placed (see (Figure 1), are added Results corresponding to the spatial distribution of IL and IL integrated on the ROI are shown in Figure 8.

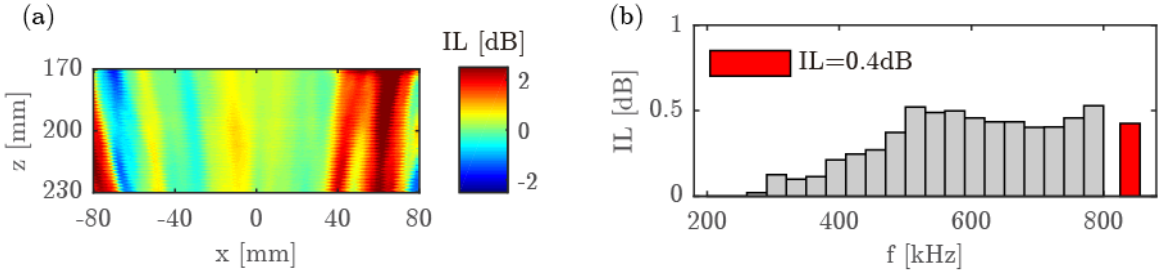

Figure 8: (a) Spatial distribution of the insertion loss (IL) and (b), IL integrated on an area of 60 × 30 mm^2, corresponding to two SCs placed symmetrically for the case shown in Figure 4(f).

First, an asymmetry with respect to the centre is observed in the results of Figure 8(a) due to some misalignment between the different elements that constitute the configuration (perforated plate, SCs, backing). Taking this into account, it is possible to identify the influence of the different elements of the configuration. In the central part of the Figure 8(a), we can observe positive values of IL which correspond to the reflection of the central part, the inner part of the channel and from the perforated flat reflector (see Figure 4 (e)). Then, the influence of the SCs is also noticeable in certain areas in the vicinity of x = +50 and x = −80, where the values of IL are positive and higher than the values in the previous part, corresponding mainly to the effect of the SCs. Although these areas are out of the ROI, it is noted that these values are consistent with the results obtained previously for the configurations using one SC (see Fig. 5(c)). Finally, Figure 8 (b) shows the parameter IL integrated over the ROI in frequency bands, and the global value integrated in space and frequency (the red bar in the right part of the plot), showing an improvement of 0.4 dB as a result of introducing two sonic crystals. This last result is a consequence of the following. As explained at the beginning of Section 2, the scaled model of the launch pad in ultrasonic regime is a good approximation in general terms, but it accounts for an important limitation, the directivity of the acoustic source is different from an acoustic source in audible regime. More precisely, in the lower frequency range of our experiments, the ultrasonic source features a high directivity. This difference does not constitute a limitation in the configurations using one SC, but it

affects the results in the configurations using two SC's, as only a small part of the incident field impinges directly on the crystals limiting their effect on the reflection, as shown in Figure 8.

4 Conclusions

In this work we present an experimental study of the use of Sonic Crystal for noise reduction at the launchpad. In particular, we have studied the VEGA's Launchpad from ESA. As a general conclusion of our analysis we can say that the use of SCs is useful for reducing the noise levels at the location of the rocket. The fact that the SCs are structured media (inhomogeneous) is at the root of the non-specular reflection responsible to this noise reduction, although other mechanisms may contribute to decrease in sound pressure levels. We have considered the effect of diffuse reflection related to a strong back-scattering of the wave in a flat reflector. However, attenuation due to thermoviscous absorption of waves in the fluid, or fluid-structure interaction, may be also present. The Insertion Loss (IL) has been the parameter used in order to compare the total field (incident plus reflected) in two different configurations. IL also measures the difference in the OASPL between the two given configurations that is a parameter usually measured in the aerospace engineering context. The SCs tested in this study have been mounted in different configurations, and in all the cases reduction of the sound levels have been observed. Our experimental study shows that the SC with triangular lattice symmetry and low filling fraction has the best noise reduction performance among all the samples.

Acknowledgements

Authors acknowledge the support of the European Space Agency under contract "Sonic Crystals For Noise Reduction At The Launch Pad" ESA ITT 1-7094 (ITI) and the 441-2015 Co-Sponsored PhD "Acoustic Reduction Methods for the Launch Pad". The work was supported by Spanish Ministry of Economy and Innovation (MINECO) and European Union FEDER through project FIS2015-65998-C2-2.

References

[1] Arenasand, J.P.; Margasahayam. R.N. Noise and vibration of spacecraft structures. *Revista chilena de acústica* 14(3), 2006, pp. 251-264

[2] Gély, D.; Elias, G. ; Mascanzoni, F.; Foulon. H. *Acoustic Environment of the VEGA Launch Vehicle at Lift-Off. Proceedings of the Forum Acusticum*, Budapest, 2005

[3] Elias, G. *Ariane 5 at lift off: localization and ranking of acoustic sources. Proceedings of the 29th International Congress and Exhibition on Noise Control Engineering,* Nice, 2000.

[4] West, J.; Strutzenberg, L. L. ; Putnam, G. C. ; Liever P. A. ; Williams B. R. *Development of Modeling Capabilities for Launch Pad Acoustics and Ignition Transient Environment Prediction. Proceedings of the 18th AIAA/CEAS Aeroacoustics Meeting Conference,* Colorado, 2012.

[5] Venkatraman, R.; Sankaran, S.; Subba Rao, S. V. ; Krishnaiah, P.; Sundararajan, T. *Investigation on the Ignition Over Pressure Related to Launch Vehicle Lift-off.* Indian Journal of Science and Technology 71(1), 2014, pp. 86-94.

[6] Vorobyov, A. M.; Abdurashidov, T. O.; Bakulev, V. L.; But, A. B.; Kuznetsov, A. B.; Makaveev, A. T. *Problem of intensity reduction of acoustic fields generated by gas-dynamic jets of motors of the rocket-launch vehicles at launch*. Acta Astronautica 109, 2015, pp. 264-268.

[7] Tsutsumi,T.; Ishii T.; Ui, K.; Tokudome, S.; Wada, K. *Study on Acoustic Prediction and Reduction of Epsilon Launch Vehicle at Liftoff.* Journal of Spacecraft And Rockets 52 (2), 2015, pp. 350-361.

[8] Moiseyenko, R. P.; Herbison, S.; Declercq, N. F.; Laude, V. *Phononic crystal diffraction gratings*. J. Appl. Phys. 111, 2012, 034907.

[9] Castiñeira-Ibáñez, S.; Romero-García, V.; Sánchez-Pérez, J. V.; García-Raffi, L. M. *Periodic Systems As Road Traffic Noise Reducing Devices: Prototype And Standardization.* Environmental Engineering and Management Journal 14 (12), 2015, pp. 2759-2769

[10] Farina A., *Simultaneous measurement of impulse response and distortion with a swept sine technique, 108th AES Convention*, Paris, 2000.